Published in final edited form as:
Mol Microbiol. 2013 March ; 87(6): 1267–1276. doi:10.1111/mmi.12165.

Characterization of *Myxococcus xanthus* MazF and Implications for a New Point of Regulation

Tye O. Boynton[a], **Jonathan L. McMurry**[b], and **Lawrence J. Shimkets**[a,†]

[a]Department of Microbiology, University of Georgia, Athens GA, 30602

[b]Department of Chemistry and Biochemstry, Kennesaw State University, Kennesaw GA, 30144

Abstract

During development, *Myxococcus xanthus* cells undergo programmed cell death (PCD) whereby 80% of vegetative cells die. Previously, the MazF RNA interferase has been implicated in this role. Recently, it was shown that deletion of the *mazF* gene does not eliminate PCD in wild-type strain DK1622 as originally seen in DZF1. To clarify the role of MazF, recombinant enzyme was characterized using a highly sensitive assay in the presence and absence of the proposed antitoxin MrpC. In contrast to previous reports that MrpC inhibits MazF activity, the hydrolysis rate was enhanced in a concentration-dependent manner with MrpC or MrpC2, an N-terminally truncated form of MrpC. Furthermore, MazF transcripts were not detected until 6–8 hours post-induction, suggesting an antitoxin is unnecessary earlier. Potential MazF targets were identified and their transcript levels were shown to decline in DK1622 while remaining steady in a *mazF* deletion strain. Elimination of the *mazF* hydrolysis site in the *nla6* transcript resulted in overproduction of the mRNA. Thus, MazF negatively regulates specific transcripts. Additionally, we show that discrepancies in the developmental phenotypes caused by removal of *mazF* in DK1622 and DZF1 are due to the presence of the *pilQ1* allele in the latter strain.

Keywords

MazF; *Myxococcus xanthus*; mRNA interferase; development

Introduction

Microbes regulate many complex processes with networks of sensing and signaling pathways. Programmed cell death (PCD) is perhaps the most intriguing because it results in altruistic suicide for the benefit of neighboring organisms (Perry *et al.*, 2009, Blower *et al.*, 2009). The δ-Proteobacterium *Myxococcus xanthus* is an excellent model for the study of cell-to-cell communication and PCD. In response to starvation, *M. xanthus* forms multicellular fruiting bodies containing spores. Development is directed by a series of extracellular signals that occur in a precise temporal order, ultimately leading to PCD for roughly 80 percent of cells (Shimkets, 1999, Wireman & Dworkin, 1977).

Recently, the *M. xanthus* genome was found to encode an orphan *mazF* toxin gene (Nariya & Inouye, 2008). Removal of *mazF* resulted in greatly reduced PCD and sporulation in strain DZF1. MazF belongs to the family of enzymes known as mRNA interferases, which function as endoribonucleases to hydrolyze RNA molecules at specific sequences

[†]Corresponding author: Lawrence J. Shimkets, Department of Microbiology, University of Georgia, Athens, GA, 30602, Voice: (706) 542-2681, Fax: (706) 542-2674, shimkets@uga.edu.

The authors declare no conflict of interest.

(Yamaguchi & Inouye, 2009). In other organisms, *mazF* is normally found cotranscribed with *mazE*. MazF activity is inhibited by MazE binding and initiated when MazE is degraded in response to stress conditions (Gerdes *et al.*, 2005). Nariya *et al.* searched for potential *M. xanthus* MazF binding partners and identified MrpC, which binds MazF *in vitro* and *in vivo* and was reported to inhibit endoribonuclease activity (Nariya & Inouye, 2008).

MrpC is a transcription factor that activates expression of many development-specific genes (Ueki & Inouye, 2003, Sun & Shi, 2001). Strains lacking *mrpC* fail to develop and sporulate (Nariya & Inouye, 2008). Pre-starvation, MrpC is negatively regulated by phosphorylation through the Pkn8/Pkn14 kinase cascade (Nariya & Inouye, 2005). Upon starvation, a shortened form of MrpC is observed that lacks the first 33 N-terminal residues, eliminating the predicted site of phosphorylation (Ueki & Inouye, 2003). Subsequent work using a recombinant form lacking only 25 N-terminal residues, named MrpC2, showed it is not present in cells lacking the protease LonD (Nariya & Inouye, 2006). Direct hydrolysis has not been demonstrated. MrpC2 binds DNA with greater affinity and positively regulates expression of *mrpC* (Nariya & Inouye, 2006). MrpC2 also binds to the promoter region upstream of the *mazF* gene to activate transcription of the *mazF* gene (Nariya & Inouye, 2008).

Together, these results point to an elegant system of PCD that is fundamentally tied to development through the use of an essential transcription factor. Unfortunately, conflicting data have recently been presented with regard to MazF function. Lee *et al.* showed that removal of *mazF* from wild-type strains DK1622 and DZ2 had little to no effect on development or PCD (Lee *et al.*, 2012). The earlier experiments had been done in the DZF1 background, which contains a *pilQ1* allele that compromises an outer membrane secretin required for S-motility (Wall *et al.*, 1999). This allele bears two missense mutations in *pilQ* that cause amino acid substitutions G741S and N762G. PilQ1 greatly sensitizes cells to antibiotics and could conceivably render cells more susceptible to PCD. Thus the role of MazF in *Myxococcus* PCD remains in question.

A larger question is whether MazF mediates PCD in any organism. MazF was initially suggested to mediate PCD in *Escherichia coli* (Aizenman *et al.*, 1996). *E. coli* MazF has a small target sequence, ACA (Zhang *et al.*, 2003). Consequently, *E. coli* MazF degrades most mRNAs, arresting protein synthesis and leading to growth arrest (Zhang et al., 2003). However, these cells can be fully revived upon induction of *mazE* and seem not undergo PCD (Pedersen *et al.*, 2002). Furthermore, MazEF was shown to contribute to cell survival and persistence in *E. coli* (Gerdes & Maisonneuve, 2012). In other organisms, specific MazF regulatory roles have been determined. *Mycobacterium tuberculosis* contains several MazF homologues, each recognizing a different pentameric sequence. Each MazF eliminates a subset of mRNAs to alter protein expression through a regulatory mechanism of specific mRNA degradation (Zhu *et al.*, 2008). In *Staphylococcus aureus*, the MazF recognition sequence is unusually abundant in virulence factor mRNA allowing induction of MazF to diminish pathogenesis (Zhu *et al.*, 2009). Similar trends of regulatory cleavage can be seen in *Clostridium difficile* and *Bacillus subtilis* (Rothenbacher *et al.*, 2012, Park *et al.*, 2011). Thus it has become apparent that MazF homologues display a wide variety of functions, none directly related to PCD. The predominant recognition sequence of *M. xanthus* MazF was determined to be an octamer, GAGUUGCA (Nariya & Inouye, 2008). Such a long recognition sequence is unique to *M. xanthus*, suggesting a specific regulatory role for the enzyme.

We employed a highly sensitive assay for MazF activity and show that recombinant MrpC and MrpC2 increase rather than inhibit recombinant MazF RNA interferase activity *in vitro*. In addition, we identify target molecules for MazF hydrolysis and show that transcript levels

are greatly diminished upon expression of MazF during development unless the MazF hydrolysis site is removed. Finally, we show that the *pilQ1* allele is responsible for stimulating PCD in DZF1 cells containing a *mazF* mutation.

Results

Expression and Purification of MazF, MrpC, and MrpC2

The *M. xanthus mazF* gene (MXAN_1659) was cloned with a N-terminal six-histidine tag. The protein was expressed and purified in *E. coli* with a yield of approximately 15 mg protein L^{-1} culture. A band corresponding to approximately 15 kDa was observed with SDS-PAGE in agreement with the theoretical molecular weight of the recombinant protein (Figure S1). No MazF proteins are known to utilize cofactors, so no distinct features were present in the UV-VIS spectrum (not shown).

The *M. xanthus mrpC* gene (MXAN_5125) was cloned and the protein expressed as a C-terminal fusion to a 55 kDa chitin binding domain with the *Saccharomyces cerevisiae* VMA intein. Cleavage of the intein with DTT yielded approximately 3 mg unmodified protein L^{-1} culture. For MrpC2, we took advantage of a natural methionine codon 75 bp downstream from the start codon of *mrpC*, which has previously been used in recombinant MrpC2 studies (Nariya & Inouye, 2006, Nariya & Inouye, 2008). MrpC2 was expressed and purified identically to MrpC with similar yields. MrpC and MrpC2 showed approximately 27 and 25 kDa bands respectively, in line with the theoretical values calculated from amino acid sequence (Figure S1). As expected, no distinct features were present in the UV-VIS spectrum.

MazF acts as a mRNA interferase

A continuous fluorometric assay was developed using an RNA oligonucleotide bearing a fluorophore at the 5'- position and a quencher at the 3'-position (Zhang *et al.*, 2005). Fluorescence is detected when this synthetic oligonucleotide is cleaved by MazF. Since the cleavage site of *M. xanthus* MazF is known (Nariya & Inouye, 2008), the substrate was designed to be 13 nucleotides long with the octamer recognition sequence (rGrArGrUrUrGrCrA) at the center.

Fluorescence was only detectable after cleavage by MazF (Figure 1A). The reaction follows standard first-order Michaelis-Menten kinetics when fitted to the Michaelis equation (Figure 1B). The K_m and V_{max} for the substrate were 62 nM and 0.4 pmol min^{-1} respectively. The maximum rate is comparable with the *E. coli* homologue having a V_{max} of 0.37 pmol min^{-1}. *M. xanthus* MazF displays a very high substrate affinity when compared to *E. coli* MazF however, which has a K_m over two orders of magnitude higher at 6.9 μM (Wang & Hergenrother, 2007).

MazF activity is enhanced, not inhibited, by MrpC/MrpC2

MazF was assayed in the presence of varying concentrations of MrpC and MrpC2 to examine potential interactions. Unexpectedly, the reaction rates were doubled in the presence of MrpC or MrpC2 (Figure 1C and 1D). With equimolar amounts of MrpC, the K_m and V_{max} of MazF became 45 nM and 0.8 pmol min^{-1}, respectively (Figure 1E). With equimolar amounts of MrpC2, the K_m and V_{max} were 42 nM and 0.7 pmol min^{-1}, respectively. Greater concentrations of MrpC or MrpC2 also enhanced the rate of hydrolysis, but with diminishing returns. For example, a ten-fold increase in MrpC:MazF ratio yielded only a four-fold increase in activity. MazF was also assayed identically in the presence of BSA to rule out the possibility that the enzymatic enhancement is nonspecific (data not shown). No stimulation was observed even at the highest BSA concentration.

mazF transcripts appear during the peak of *mrpC* levels

Expression of MrpC increases 6–12 hours post-starvation, when MrpC2 first appears (Nariya & Inouye, 2005). MrpC2 increases *mrpC* expression during this time by binding to its own promoter region with a 4-fold higher affinity than MrpC (Nariya & Inouye, 2006). Two putative MrpC binding sequences are also present in the *mazF* promoter region leading one to suspect that MazF is produced in the same time frame (Nariya & Inouye, 2008). The relative transcript levels of *mazF* and *mrpC* were determined via quantitative RT-PCR in the wild-type strain DK1622 at 2, 4, 6, 8, 12, and 24 hours post-starvation, with each timepoint normalized against the housekeeping gene *rpoC* (MXAN_3078). The 0 hour samples represent transcript levels present during vegetative growth. *mrpC* transcript levels are in agreement with Western blots that show MrpC levels peaking around 12 hours followed by a sharp decline (Konovalova *et al.*, 2012) (Figure 2). In DK1622, *mazF* transcripts could not be detected until 6–8 hours, peaking around 12 hours. These data indicate that MazF is a development-specific protein.

MazF regulates transcript levels of genes required for development and cell viability

MazF cannot compromise global transcript levels due to the specificity of the *M. xanthus* MazF recognition sequence. To address what portions of the transcriptome are altered *in vivo*, Pattern Locator (http://www.cmbl.uga.edu/software/patloc.html) was used to generate a list of coding sequences containing the cleavage site 5'-GAGUUGCA-3' (Mrazek & Xie, 2006) (Table S1). Five potential candidates were selected from the list of 72 due to their ability to alter cell fate or mediate development (highlighted on table S1). *nuoM* encodes the M subunit of NADH dehydrogenase, a complex required for stationary phase survival in *E. coli* and many other organisms (Zambrano & Kolter, 1993). ClpA is part of the multimeric ClpAP protease, which mediates protein degradation and is also required for *E. coli* stationary phase survival (Weichart *et al.*, 2003). The remaining three genes are required for *M. xanthus* development. FrzZ is the output of the Frz chemosensory pathway and is required for fruiting body formation (Inclan *et al.*, 2007). EpsE is a glycosyl transferase involved in exopolysaccharide biosynthesis and is required for S-motility and fruiting body formation (Lu *et al.*, 2005). Nla6 is an enhancer protein that is required for sporulation (Caberoy *et al.*, 2003). It should be noted that the list of genes presented in Table S1 may not contain all MazF targets, as cleavage of any of these transcripts may also affect translation of other genes within the same transcript. Intergenic regions were not included but could produce as yet unidentified small RNAs.

RT-PCR was used to quantify relative transcript levels 2, 4, 6, 8, 12, and 24 hours post-starvation in DK1622 and LS3118 (Δ*mazF*) (Figure 3). All five MazF target transcripts peaked 4–6 hours after development. They dropped off in DK1622 but remained high in cells lacking MazF. A gene lacking the MazF hydrolysis site, *fmgD* (MXAN_1501), was also examined and had identical profiles in both wild type and LS3118 (Figure 3).

To prove that MazF is directly responsible for the changes in target mRNA levels, LS3160 was created in which *nla6* was desensitized to MazF. Two silent mutations were introduced, T751C and G753C, abolishing the MazF hydrolysis site but maintaining the amino acid sequence. Transcript levels were found to remain high despite the presence MazF, confirming the biological relevance of MazF in reducing these transcripts (Figure 4).

The *pilQ1* allele blocks development in *mazF* mutants

Removal of *mazF* from the *M. xanthus* genome has a deleterious effect on development of DZF1, but not in the wild type strains DK1622 and DZ2 (Lee *et al.*, 2012). Of the many differences in DZF1, one key mutation is the *pilQ1* allele, which renders *M. xanthus* incapable of social motility and nearly 1000-fold more susceptible to certain lethal

substances such as vancomycin (Wall *et al.*, 1999). A DK1622 derived strain called LS3143 bearing *pilQ1* and Δ*mazF* was created to examine whether it would recreate the developmental defect observed with DZF1. Fruiting body formation and sporulation were compared with DK1622, DK8611 (DK1622 bearing the *pilQ1* allele of DZF1), and LS3118 (Δ*mazF*) (Figure 5). DK1622, DK8611, and LS3118 were all competent in fruiting body formation and sporulation. In contrast, LS3143 was unable to form fruiting bodies or spores, mimicking the characteristics reported for a *mazF* deletion in DZF1.

Discussion

During *M. xanthus* development roughly 80% of the population is sacrificed by PCD. Neither the mechanism of PCD, nor the method by which cells acquire a specific fate are understood. The recent discovery of MazF in *M. xanthus* suggested a model whereby the mRNA interferase remained inactive via a complex with the transcription factor MrpC. In this model, MrpC is degraded by proteases, allowing MazF to stimulate lysis. However, while MazF is necessary for PCD and sporulation in strain DZF1, it is not essential for PCD or sporulation in wild type strains DK1622 and DZ2. Thus, we reexamined the function of MazF.

Our data shows enhancement of MazF endoribonuclease activity by MrpC and MrpC2 in direct opposition to the inhibition reported previously by Nariya and Inouye. One possible explanation for this is the type of assay used in the respective experiments. Whereas the previous observations used a qualitative gel electrophoresis assay that relied on the cleavage of MS2 ssRNA (Nariya & Inouye, 2008), we used a sensitive, continuous fluorometric assay with an artificial target with the *M. xanthus* MazF hydrolysis site. Another source of variation is the recombinant proteins. In the Nariya and Inouye study, MazF, MrpC, and MrpC2 are expressed with 22 amino acid, N-terminal additions containing 10× histidine tags. While our MazF has a 12 amino acid N-terminal addition containing a 6× histidine tag, our MrpC and MrpC2 proteins do not contain additional sequences and should more closely mimic the native proteins.

The hydrolysis site of *M. xanthus* MazF is an octamer found in only about 1% of *M. xanthus* genes. In organisms where the recognition sequence is 4–5 nucleotides, such as *S. aureus* and *M. tuberculosis*, MazF negatively regulates the expression of a subset of genes (Zhu *et al.*, 2008, Zhu *et al.*, 2009). Thus it is likely that *M. xanthus* MazF functions similarly, with a much greater specificity. Our data show that MazF degrades a subset of mRNAs, a few of which are tied to cell viability and development. Of the five genes selected from the list of potential targets, all were reduced *in vivo*, some below levels found in vegetative cells. Through these genes and other potential targets, MazF regulates synthesis of proteins at the posttranscriptional level.

Unlike the previous model of MazF action (Nariya & Inouye, 2008), our data point to a model in which MazF functions without an antitoxin (Figure 6). In vegetative cells, MrpC is sequestered into an inactive state through a previously established protein kinase cascade whereby Pkn14 phosphorylates MrpC. With MrpC phosphorylated and unable to bind the *mazF* promoter, MazF is not expressed at appreciable levels. Once development is initiated, MrpC is hydrolyzed to MrpC2 by a process requiring LonD protease and is no longer able to be phosphorylated (Nariya & Inouye, 2006). Cleavage through LonD may constitute a bistable switch, as conversion to MrpC2 positively regulates production of MrpC. Now active, MrpC2 upregulates its own transcription and initiates transcription of *mazF*, which then negatively regulates mRNA transcript levels. Interestingly, *Myxococcus* has recruited its own transcriptional activator as an enhancer of enzymatic activity. This novel mode of

action for MazF means that MrpC regulates MazF at both the transcriptional and post-translational levels.

Deletion of *mazF* causes different phenotypes in different genetic backgrounds. From the DZF1 data, it would appear that MazF is required for PCD (Nariya & Inouye, 2008). In DK1622 and DZ2, however, *mazF* mutant cells develop and sporulate virtually identical to their parental strains (Lee *et al.*, 2012). The phenotypic effects of *mazF* removal in DZF1 were recreated in DK1622 by introducing the *pilQ1* mutation into a Δ*mazF* mutant. Two possible explanations are apparent. As proposed by Lee *et al.*, two parallel, redundant pathways of PCD could exist in DK1622 and DZ2, one controlled by MazF, and the other by an as yet unknown mechanism disrupted in DZF1. Removal of *mazF* in the strain would then be deleterious to development. Alternatively, the observed phenotypic differences may be more artifactual than revealing, and result from the increased sensitivity of the *pilQ1* allele to toxic molecules. *pilQ1* results in a 1000-fold increased sensitivity to vancomycin suggesting that the porin is held in an open state. The increased membrane permeability coupled with removal of MazF activity could then indirectly affect cell fate independent of PCD. Further experimentation is required to distinguish between these possibilities.

In conclusion, *M. xanthus* MazF RNA interferase controls expression of roughly 1% of the genome by a novel mechanism involving stimulation by its transcription factor MrpC. This represents the first description of a so-called toxin devoid of its corresponding antitoxin. These results further support the idea that MazF proteins are not global toxins, but instead play regulatory roles distinct to each organism.

Experimental Procedures

Bacterial Strains and Plasmids and Development of *Myxococcus xanthus*

All strain and plasmids used in this study are listed in Table 1. Sequences of all PCR primers can be found in table S2. Unless noted, *M. xanthus* and *E. coli* strains were grown in CYE (1.0% Bacto Casitone, 0.5% Difco yeast extract, 10 mM 3-[N-morpholino] propanesulfonic acid, pH 7.6, and 0.1% $MgSO_4$) and LB respectively, and supplemented with 50 μg ml^{-1} kanamycin and 50 μg ml^{-1} ampicillin where appropriate. *M. xanthus* and *E. coli* were grown at 32°C and 37°C respectively. Development of *M. xanthus* was induced by first growing cells to a concentration of 5×10^8 cells ml^{-1} in CYE with shaking. Cells were pelleted and then resuspended in sterile water at 5×10^9 cells ml^{-1}. 20 μl of this suspension was then spotted onto TPM agar (10 mM Tris-HCl, 8 mM $MgSO_4$, 1 mM K_2HPO_4-KH_2PO_4, 1.5% Difco agar, pH 7.6) and incubated at 32°C. For quantification of spores, spots were resuspended 5 days post-starvation in 1 ml dH_20 and incubated 55 °C for one hour followed by brief sonication to kill vegetative cells. Spores were then counted directly using a Petroff-Hauser chamber.

Strain LS3118 (Δ*mazF*) was generated through the double recombination method as previously described (Ueki *et al.*, 1996) using the vector pBJ113 (Julien *et al.*, 2000). Briefly, plasmid pTOB12 was synthesized by Genscript (Piscataway, NJ, USA) to contain the 700 bp immediately upstream of the *M. xanthus mazF* (MXAN_1659) coding sequence fused to the 700 bp immediately downstream. This 1400 bp fragment was flanked by 5' KpnI and 3' HindIII restriction sequences and inserted into the *EcoRV* site of pUC57. pTOB12 was then digested with KpnI and HindIII and the 1400 bp insert was ligated into the respective sites of the plasmid vector pBJ113 to create pTOB13. This plasmid was then transformed into electrocompetent DK1622 cells with selection for kanamycin resistance where it integrated by a single homologous crossover. A second recombination event was counterselected with CYE containing 1% galactose and resulted in an in-frame deletion that was identified by PCR.

Strain LS3160 was created using the double recombination method above with pTOB30. pTOB30 was created by first amplifying nucleotides 1–747 of *nla6*, adding a 5' KpnI site and 3' SacI site. Nucleotides 754–1455 were also amplified adding a 5' SacI site and 3' HindIII site. Ligation of these two products into the KpnI site and HindIII site of pBJ113 yielded a plasmid in which the SacI site changed nucleotides 748–753 of *nla6* from 5'-GAGTTG-3' to 5'-GAGCTC-3', introducing the silent mutations T751C and G753C.

Strain LS3143 was generated by transduction of the *pilQ1* allele from DK8611 into LS3118 via bacteriophage Mx4 (Campos *et al.*, 1978).

For the *mazF* expression vector pTOB2, pTOB1 was first synthesized by Genscript (Piscataway, NJ, USA) to contain *M. xanthus mazF* codon-optimized for *E. coli* flanked by 5' NheI and 3' HindIII restriction sequences. The insert was removed and ligated into the respective sites of pTrcHisB (Invitrogen, Grand Island, NY, USA). The codon optimized sequenced of pTOB1 can be seen in Figure S2 and lacks the natural start codon. The protein product contains a 12 N-terminal amino acid addition including a 6× His tag.

For the *mrpC* expression vector pTOB14, the *M. xanthus mrpC* sequence was codon-optimized (Figure S3) and synthesized as before to obtain plasmid pTOB7. Optimized *mrpC* was amplified by PCR from pTOB7 to contain no stop codon and flanking 5' NdeI and 3' XhoI restriction sites. The amplicon was ligated into the respective sites of the commercial vector pTYB2 (New England Biolabs, Ipswich, MA, USA). pTOB15 was generated in a similar fashion, except that the amplified PCR product lacked the first 75 bp of the optimized *mrpC* gene using a natural ATG at this position as a start codon (Nariya & Inouye, 2006). The protein products of pTOB14 and pTOB15 were designed so that intein self-splicing generates products with the native amino acid sequences.

Expression and Purification of Recombinant Proteins

Expression and purification of MazF was performed as previously described (Boynton *et al.*, 2009). Briefly, *E. coli* bearing pTOB2 were grown for 6 hours at 30°C in 100 mL Circlegrow media (MP Biomedicals, Solon, OH, USA) containing 50 μg ml^{-1} ampicillin and then transferred to 1 L of Circlegrow media and grown for an additional 22 hours at 30°C. Cells collected by centrifugation were lysed by sonication in a solubilization buffer containing 50 mM Tris-buffer 3-(N-Morpholino) propane-sulfonic acid (MOPS) pH 8.0, 100 mM KCl, 1% sodium cholate, and 10 μg ml^{-1} phenylmethylsulfonyl fluoride (PMSF). The lysate was then centrifuged for 30 minutes at 100,000 × g and the resulting supernatant applied to a column containing 1.25 mL bed volume HisPur Cobalt Affinity Resin (Thermo Scientific, Rockford, IL, USA). The column was then washed with 20 bed volumes solubilization buffer. Recombinant protein was eluted in 1 mL fractions of solubilization buffer containing 300 mM imidazole.

E. coli bearing pTOB14 or pTOB15 plasmids were grown overnight at 37°C and used to inoculate 1L LB containing ampicillin the following morning. When the culture density reached 0.6 OD_{600}, protein expression was induced with 0.4 mM IPTG for 24 hrs. Cells were harvested and then sonicated in STE buffer [20 mM Tris-Cl (pH 8.0), 500 mM NaCl, and 0.1 mM EDTA]. The lysate was ultracentrifuged as above and the resulting supernatant applied to a column containing 2.5 mL bed volumes of chitin beads (New England Biolabs, Ipswich, MA, USA). The column was then washed with 20 mL STE buffer. To elute, 5 mL cleavage buffer [20 mM Tris-HCl (pH 8.0), 50 mM NaCl, 0.1 mM EDTA, and 50 mM dithiothreitol] were loaded onto the column and allowed to incubate overnight at 4°C. Recombinant proteins were then eluted. All proteins were quantified using UV/VIS spectrophotometry from the absorption peak of a protein scan using predicted extinction coefficients. Proteins were visualized by sodium dodecyl sulfate-polyacrylamide gel

electrophoresis (SDS-PAGE) using Bio-Rad 4–20% Tris-HCl ready-made gels (Bio-Rad, Hercules, CA, USA).

Continuous Fluorometric Assay

MazF activity was assayed as previously described (Wang & Hergenrother, 2007) with modifications, using the following labeled oligonucleotude substrate obtained from IDT (Coraville, IA, USA): 6-carboxyfluorescein (6-FAM)-5'-rArArGrArGrUrUrGrCrArCrArG-3'-Black Hole Quencher 1 (BHQ1). Reaction mixtures consisted of 5 mM Tris-HCl (pH 8.0), 0.5 mM EDTA, 250 nM MazF, and varying amounts of substrate, MrpC, and MrpC2 where appropriate. Rates were monitored as a function of fluorescence emitted upon cleavage of substrate. Experiments were conducted at 32°C with shaking, using a Synergy 2 HTI plate reader (BioTek, Winooski, VT, USA) equipped with 485 ± 15 nm excitation filter and 530 ± 15 nm emission filter. For kinetics, data were fitted to eq 1:

$$v = V_{max}[S]/(K_m + [S])$$

where V_{max} is the apparent maximum rate and K_m is the apparent Michaelis-Menton constant.

Quantification of Transcript Level Changes During Development

To determine mRNA transcript levels of target genes, RNA was extracted at time points during development from DK1622, LS3118,or LS3160. Samples collected at different time points after induction of development were subjected to RNA extraction using the RNASNAP method followed by standard ethanol precipitation (Stead *et al.*, 2012). Quantification of transcript levels was done using the iScript One-Step RT-PCR Kit With SYBR Green (Bio-Rad, Hercules, CA, USA) and carried out with the iCycler iQ Realtime PCR Detection System (Bio-Rad, Hercules, CA, USA) with the following reaction cycle: 50°C for 10 minutes, 95°C for 5 minutes, then 45 cycles of 95°C for 10 seconds, 55°C for 30 seconds, and 72°C for 30 seconds. Meltcurve analysis was carried out at 55–95°C for 10 seconds, increasing the temperature 0.5°C each cycle for 80 cycles. Relative fold-changes in transcript levels were calculated using the ΔΔCT method and expressed as log2 inductions (Livak & Schmittgen, 2001), normalized against the housekeeping gene, *rpoC* (MXAN_3078). Primers sequences are listed in table S2.

Supplementary Material

Refer to Web version on PubMed Central for supplementary material.

Acknowledgments

The authors would like to thank Dan Wall for providing strain DK8611.

Research reported in this publication was supported by the National Institute of General Medical Science of the National Institutes of Health under award number R01GM095826 and by the Natural Science Foundation under award number MCB0742976.

References

Aizenman E, Engelberg-Kulka H, Glaser G. An *Escherichia coli* chromosomal "addiction module" regulated by guanosine [corrected] 3',5'-bispyrophosphate: a model for programmed bacterial cell death. Proc Natl Acad Sci U S A. 1996; 93:6059–6063. [PubMed: 8650219]

Amann E, Brosius J, Ptashne M. Vectors bearing a hybrid trp-lac promoter useful for regulated expression of cloned genes in *Escherichia coli*. Gene. 1983; 25:167–178. [PubMed: 6363212]

Blower TR, Fineran PC, Johnson MJ, Toth IK, Humphreys DP, Salmond GP. Mutagenesis and functional characterization of the RNA and protein components of the toxIN abortive infection and toxin-antitoxin locus of *Erwinia*. J Bacteriol. 2009; 191:6029–6039. [PubMed: 19633081]

Boynton TO, Daugherty LE, Dailey TA, Dailey HA. Identification of *Escherichia coli* HemG as a novel, menadione-dependent flavodoxin with protoporphyrinogen oxidase activity. Biochemistry. 2009; 48:6705–6711. [PubMed: 19583219]

Caberoy NB, Welch RD, Jakobsen JS, Slater SC, Garza AG. Global mutational analysis of NtrC-like activators in *Myxococcus xanthus*: identifying activator mutants defective for motility and fruiting body development. J Bacteriol. 2003; 185:6083–6094. [PubMed: 14526020]

Campos JM, Geisselsoder J, Zusman DR. Isolation of bacteriophage MX4, a generalized transducing phage for *Myxococcus xanthus*. J Mol Biol. 1978; 119:167–178. [PubMed: 416222]

Chen H, Keseler IM, Shimkets LJ. Genome size of *Myxococcus xanthus* determined by pulsed-field gel electrophoresis. J Bacteriol. 1990; 172:4206–4213. [PubMed: 2165472]

Chong S, Mersha FB, Comb DG, Scott ME, Landry D, Vence LM, Perler FB, Benner J, Kucera RB, Hirvonen CA, Pelletier JJ, Paulus H, Xu MQ. Single-column purification of free recombinant proteins using a self-cleavable affinity tag derived from a protein splicing element. Gene. 1997; 192:271–281. [PubMed: 9224900]

Durfee T, Nelson R, Baldwin S, Plunkett G 3rd, Burland V, Mau B, Petrosino JF, Qin X, Muzny DM, Ayele M, Gibbs RA, Csorgo B, Posfai G, Weinstock GM, Blattner FR. The complete genome sequence of *Escherichia coli* DH10B: insights into the biology of a laboratory workhorse. J Bacteriol. 2008; 190:2597–2606. [PubMed: 18245285]

Gerdes K, Christensen SK, Lobner-Olesen A. Prokaryotic toxin-antitoxin stress response loci. Nat Rev Microbiol. 2005; 3:371–382. [PubMed: 15864262]

Gerdes K, Maisonneuve E. Bacterial persistence and toxin-antitoxin loci. Annu Rev Microbiol. 2012; 66:103–123. [PubMed: 22994490]

Inclan YF, Vlamakis HC, Zusman DR. FrzZ, a dual CheY-like response regulator, functions as an output for the Frz chemosensory pathway of *Myxococcus xanthus*. Mol Microbiol. 2007; 65:90–102. [PubMed: 17581122]

Julien B, Kaiser AD, Garza A. Spatial control of cell differentiation in *Myxococcus xanthus*. Proc Natl Acad Sci U S A. 2000; 97:9098–9103. [PubMed: 10922065]

Konovalova A, Wegener-Feldbrugge S, Sogaard-Andersen L. Two intercellular signals required for fruiting body formation in *Myxococcus xanthus* act sequentially but non-hierarchically. Mol Microbiol. 2012; 86:65–81. [PubMed: 22834948]

Lee B, Holkenbrink C, Treuner-Lange A, Higgs PI. *Myxococcus xanthus* developmental cell fate production: heterogeneous accumulation of developmental regulatory proteins and reexamination of the role of MazF in developmental lysis. J Bacteriol. 2012; 194:3058–3068. [PubMed: 22493014]

Livak KJ, Schmittgen TD. Analysis of relative gene expression data using real-time quantitative PCR and the 2(-Delta Delta C(T)) Method. Methods. 2001; 25:402–408. [PubMed: 11846609]

Lu A, Cho K, Black WP, Duan XY, Lux R, Yang Z, Kaplan HB, Zusman DR, Shi W. Exopolysaccharide biosynthesis genes required for social motility in *Myxococcus xanthus*. Mol Microbiol. 2005; 55:206–220. [PubMed: 15612929]

Mrazek J, Xie S. Pattern locator: a new tool for finding local sequence patterns in genomic DNA sequences. Bioinformatics. 2006; 22:3099–3100. [PubMed: 17095514]

Nariya H, Inouye M. MazF, an mRNA interferase, mediates programmed cell death during multicellular *Myxococcus* development. Cell. 2008; 132:55–66. [PubMed: 18191220]

Nariya H, Inouye S. Identification of a protein Ser/Thr kinase cascade that regulates essential transcriptional activators in *Myxococcus xanthus* development. Mol Microbiol. 2005; 58:367–379. [PubMed: 16194226]

Nariya H, Inouye S. A protein Ser/Thr kinase cascade negatively regulates the DNA-binding activity of MrpC, a smaller form of which may be necessary for the *Myxococcus xanthus* development. Mol Microbiol. 2006; 60:1205–1217. [PubMed: 16689796]

Park JH, Yamaguchi Y, Inouye M. *Bacillus subtilis* MazF-bs (EndoA) is a UACAU-specific mRNA interferase. FEBS Lett. 2011; 585:2526–2532. [PubMed: 21763692]

Pedersen K, Christensen SK, Gerdes K. Rapid induction and reversal of a bacteriostatic condition by controlled expression of toxins and antitoxins. Mol Microbiol. 2002; 45:501–510. [PubMed: 12123459]

Perry JA, Cvitkovitch DG, Levesque CM. Cell death in *Streptococcus mutans* biofilms: a link between CSP and extracellular DNA. FEMS Microbiol Lett. 2009; 299:261–266. [PubMed: 19735463]

Rothenbacher FP, Suzuki M, Hurley JM, Montville TJ, Kirn TJ, Ouyang M, Woychik NA. *Clostridium difficile* MazF toxin exhibits selective, not global, mRNA cleavage. J Bacteriol. 2012; 194:3464–3474. [PubMed: 22544268]

Shimkets LJ. Intercellular signaling during fruiting-body development of *Myxococcus xanthus*. Annu Rev Microbiol. 1999; 53:525–549. [PubMed: 10547700]

Stead MB, Agrawal A, Bowden KE, Nasir R, Mohanty BK, Meagher RB, Kushner SR. RNAsnap: a rapid, quantitative and inexpensive, method for isolating total RNA from bacteria. Nucleic Acids Res. 2012; 40:e156. [PubMed: 22821568]

Sun H, Shi W. Genetic studies of *mrp*, a locus essential for cellular aggregation and sporulation of *Myxococcus xanthus*. Journal of bacteriology. 2001; 183:4786–4795. [PubMed: 11466282]

Ueki T, Inouye S. Identification of an activator protein required for the induction of *fruA*, a gene essential for fruiting body development in *Myxococcus xanthus*. Proc Natl Acad Sci U S A. 2003; 100:8782–8787. [PubMed: 12851461]

Ueki T, Inouye S, Inouye M. Positive-negative KG cassettes for construction of multi-gene deletions using a single drug marker. Gene. 1996; 183:153–157. [PubMed: 8996101]

Wall D, Kolenbrander PE, Kaiser D. The *Myxococcus xanthus pilQ (sglA)* gene encodes a secretin homolog required for type IV pilus biogenesis, social motility, and development. J Bacteriol. 1999; 181:24–33. [PubMed: 9864308]

Wang NR, Hergenrother PJ. A continuous fluorometric assay for the assessment of MazF ribonuclease activity. Anal Biochem. 2007; 371:173–183. [PubMed: 17706586]

Weichart D, Querfurth N, Dreger M, Hengge-Aronis R. Global role for ClpP-containing proteases in stationary-phase adaptation of *Escherichia coli*. J Bacteriol. 2003; 185:115–125. [PubMed: 12486047]

Wireman JW, Dworkin M. Developmentally induced autolysis during fruiting body formation by *Myxococcus xanthus*. J Bacteriol. 1977; 129:798–802. [PubMed: 402359]

Yamaguchi Y, Inouye M. mRNA interferases, sequence-specific endoribonucleases from the toxin-antitoxin systems. Prog Mol Biol Transl Sci. 2009; 85:467–500. [PubMed: 19215780]

Yanisch-Perron C, Vieira J, Messing J. Improved M13 phage cloning vectors and host strains: nucleotide sequences of the M13mp18 and pUC19 vectors. Gene. 1985; 33:103–119. [PubMed: 2985470]

Zambrano MM, Kolter R. *Escherichia coli* mutants lacking NADH dehydrogenase I have a competitive disadvantage in stationary phase. J Bacteriol. 1993; 175:5642–5647. [PubMed: 8366049]

Zhang Y, Zhang J, Hara H, Kato I, Inouye M. Insights into the mRNA cleavage mechanism by MazF, an mRNA interferase. J Biol Chem. 2005; 280:3143–3150. [PubMed: 15537630]

Zhang Y, Zhang J, Hoeflich KP, Ikura M, Qing G, Inouye M. MazF cleaves cellular mRNAs specifically at ACA to block protein synthesis in *Escherichia coli*. Mol Cell. 2003; 12:913–923. [PubMed: 14580342]

Zhu L, Inoue K, Yoshizumi S, Kobayashi H, Zhang Y, Ouyang M, Kato F, Sugai M, Inouye M. *Staphylococcus aureus* MazF specifically cleaves a pentad sequence, UACAU, which is unusually abundant in the mRNA for pathogenic adhesive factor SraP. J Bacteriol. 2009; 191:3248–3255. [PubMed: 19251861]

Zhu L, Phadtare S, Nariya H, Ouyang M, Husson RN, Inouye M. The mRNA interferases, MazF-mt3 and MazF-mt7 from *Mycobacterium tuberculosis* target unique pentad sequences in single-stranded RNA. Mol Microbiol. 2008; 69:559–569. [PubMed: 18485066]

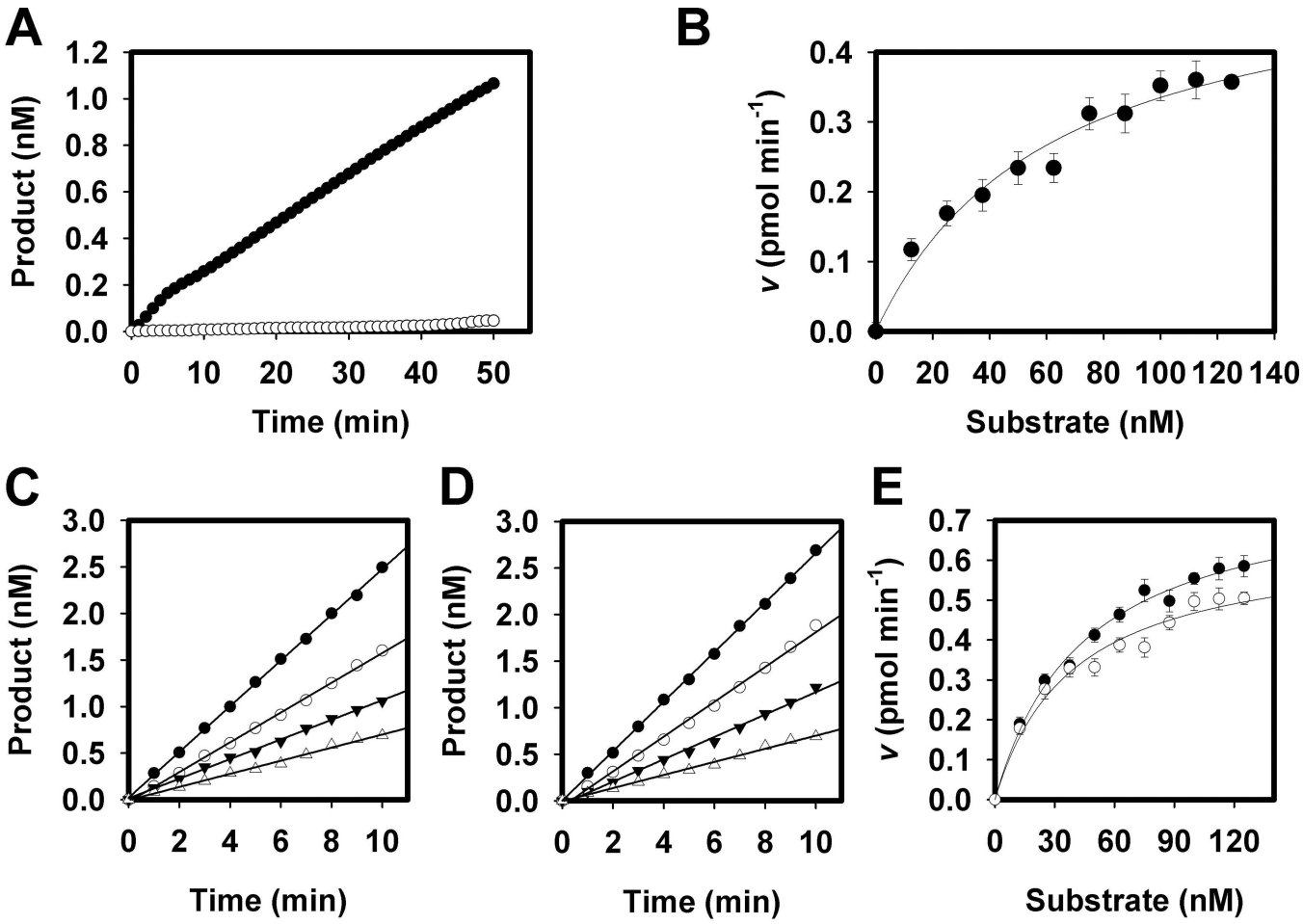

Figure 1.

Enzymatic hydrolysis of synthetic substrate by MazF. **A.** MazF mRNA interferase assays are shown for 250 nM MazF + 25 nM substrate (6-carboxyfluorescein 5'-rArArGrArGrUrUrGrCrArCrArG-3'-Black Hole Quencher 1) (●) versus substrate only (○). Activity is only seen in the presence of enzyme. **B.** Determination of apparent Michaelis constants for MazF. 250 nM MazF was assayed in the presence of varying concentrations of substrate. Data were fitted to equation 1. The K_m and V_{max} were 62 nM and 0.4 pmol min^{-1} respectively. Error bars represent the standard deviation of triplicate experiments. **C–E.** Enzymatic activity of MazF is enhanced in the presence of MrpC or MrpC2. **C**. Sample assay of 250 nM MazF alone (△) or in the presence of 250 nM (▼), 2.5 μM (○), or 25 μM (●) MrpC. **D**. Sample assay of 250 nM MazF alone (△) or in the presence of 250 nM (▼), 2.5 μM (○), or 25 μM (●) MrpC2. **E.** Effect of MrpC and MrpC2 on Michaelis constants for the MazF reaction. Equimolar amounts of MrpC (○) or MrpC2 (●) were used. V_{max} and K_m for 250 nM MazF + 250 nM MrpC were 45 nM and 0.8 pmol min^{-1} respectively. V_{max} and K_m for 250 nM MazF + 250 nM MrpC2 were 42 nM and 0.7 pmol min^{-1} respectively. Error bars represent the standard deviation of triplicate experiments.

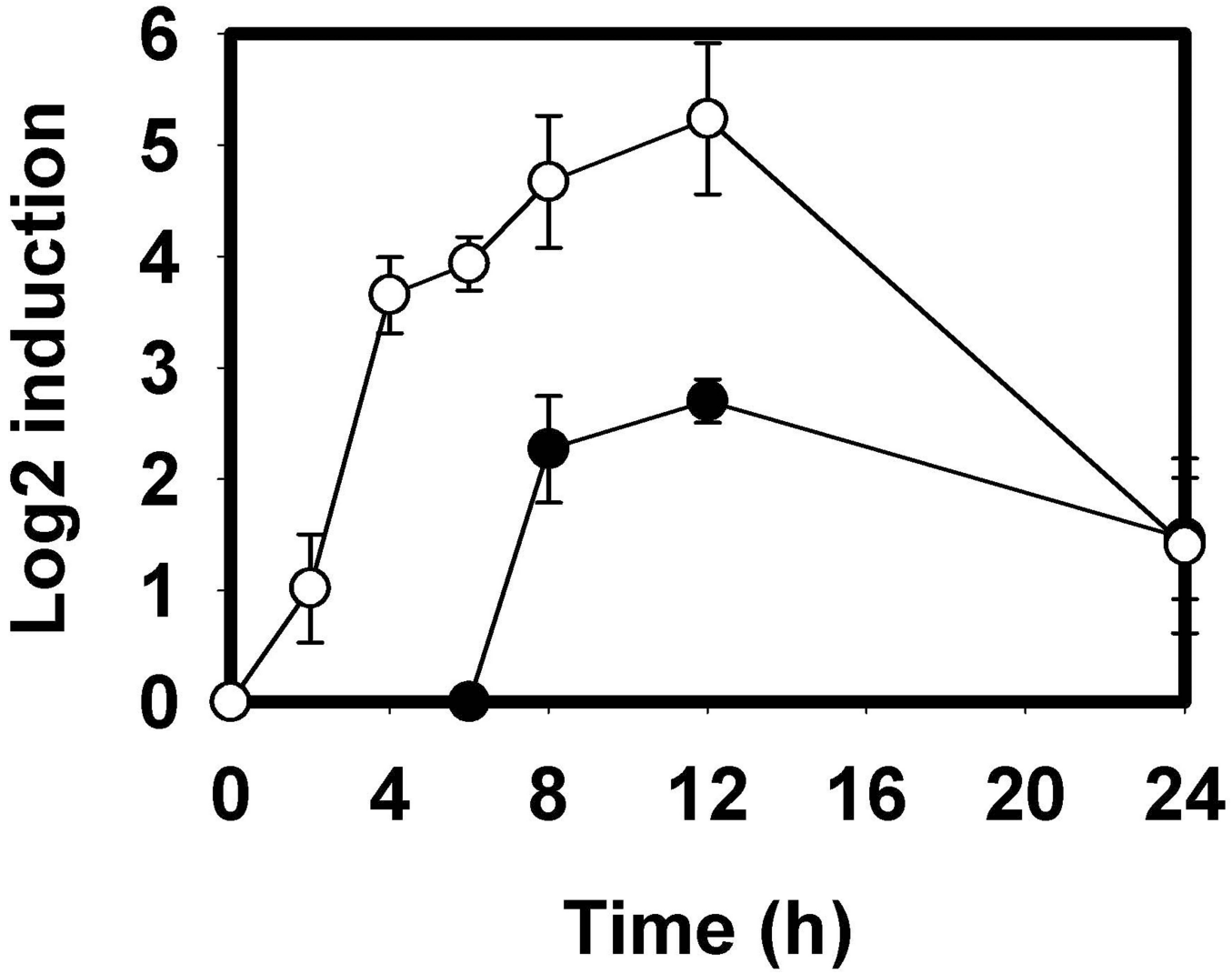

Figure 2.

Relative transcript levels of *mrpC* and *mazF* during development. Transcript levels of *mrpC* (○) and *mazF* (●) were determined using quantitative RT-PCR during 2, 4, 6, 8, 12, and 24 hour time points post-starvation compared with vegetative cells. *mazF* transcripts were not detected until 6–8 hours, during the peak of *mrpC* expression. Relative levels were calculated using the ΔΔCT method with error bars representing the standard deviation of triplicate samples.

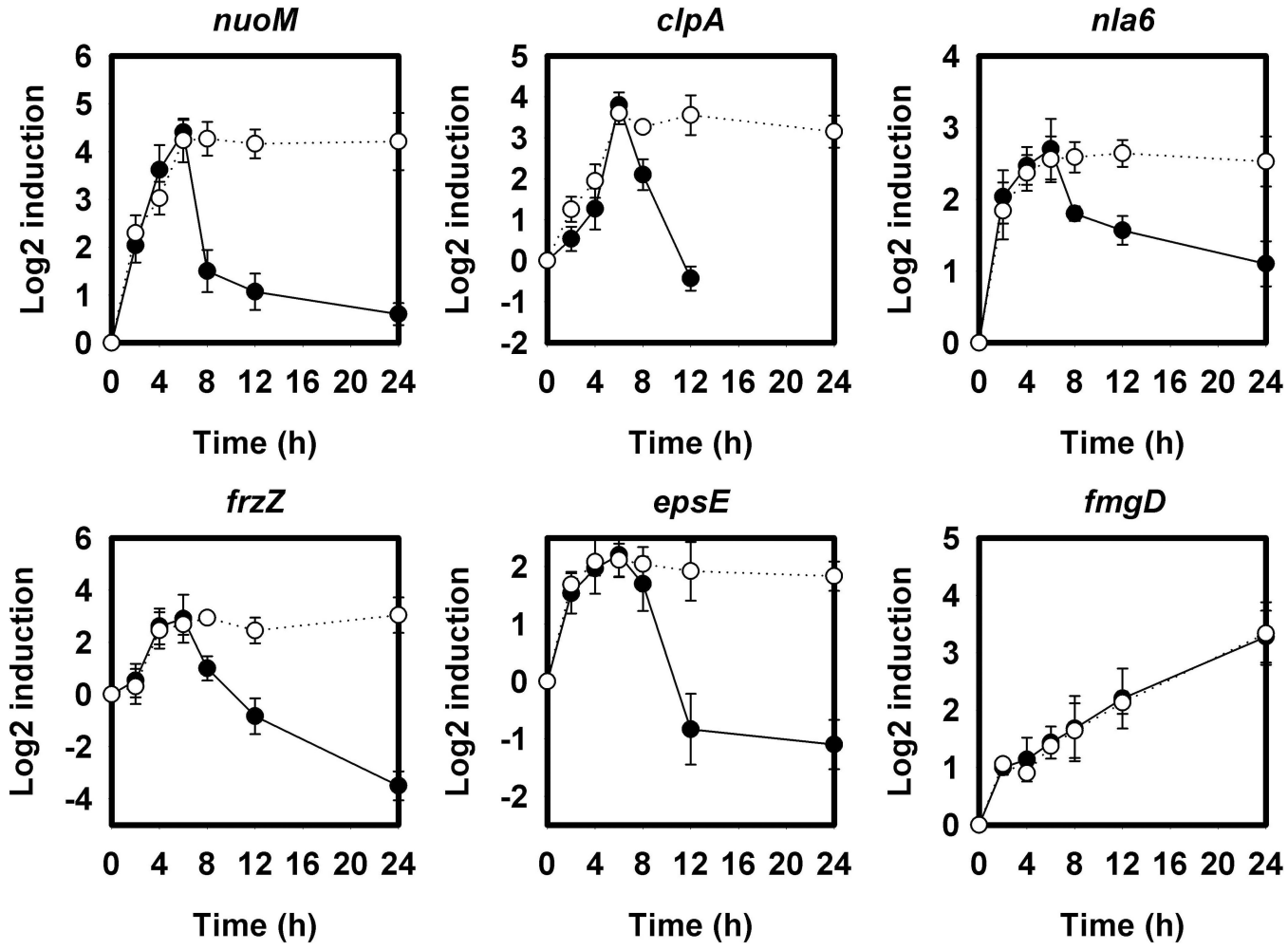

Figure 3.

Relative transcript levels of potential MazF targets during development. Transcript levels were determined as in Figure 2 for each of the 5 candidate genes in wild type DK1622 (●) and the Δ*mazF* strain LS3118 (○). In cells containing MazF, transcripts of each of these genes began to drop significantly around 8 hours at the time MazF is expressed, unlike LS3118. *fmgD* lacks the MazF recognition sequence and was used as a control. Relative levels were calculated using the ΔΔCT method with error bars representing the standard deviation of triplicate samples.

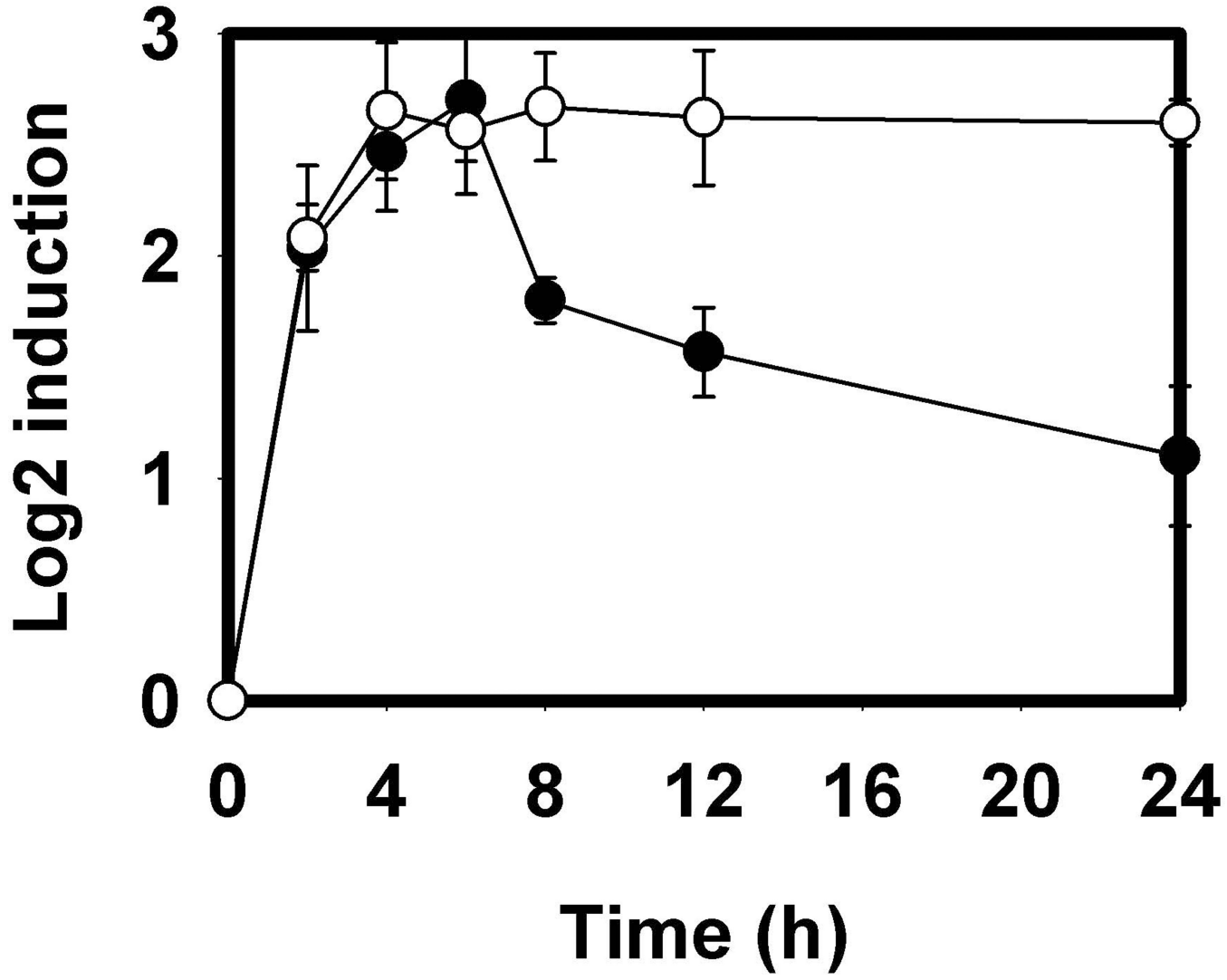

Figure 4.

Decreased levels of MazF target mRNA is enzyme-specific. Relative transcript levels of wild type *nla6* mRNA (●) decrease during development while LS3160 (○) do not. LS3160 contains two silent mutations in *nla6* that abolish the MazF hydrolysis site. Relative levels were calculated using the ΔΔCT method with error bars representing the standard deviation of triplicate samples.

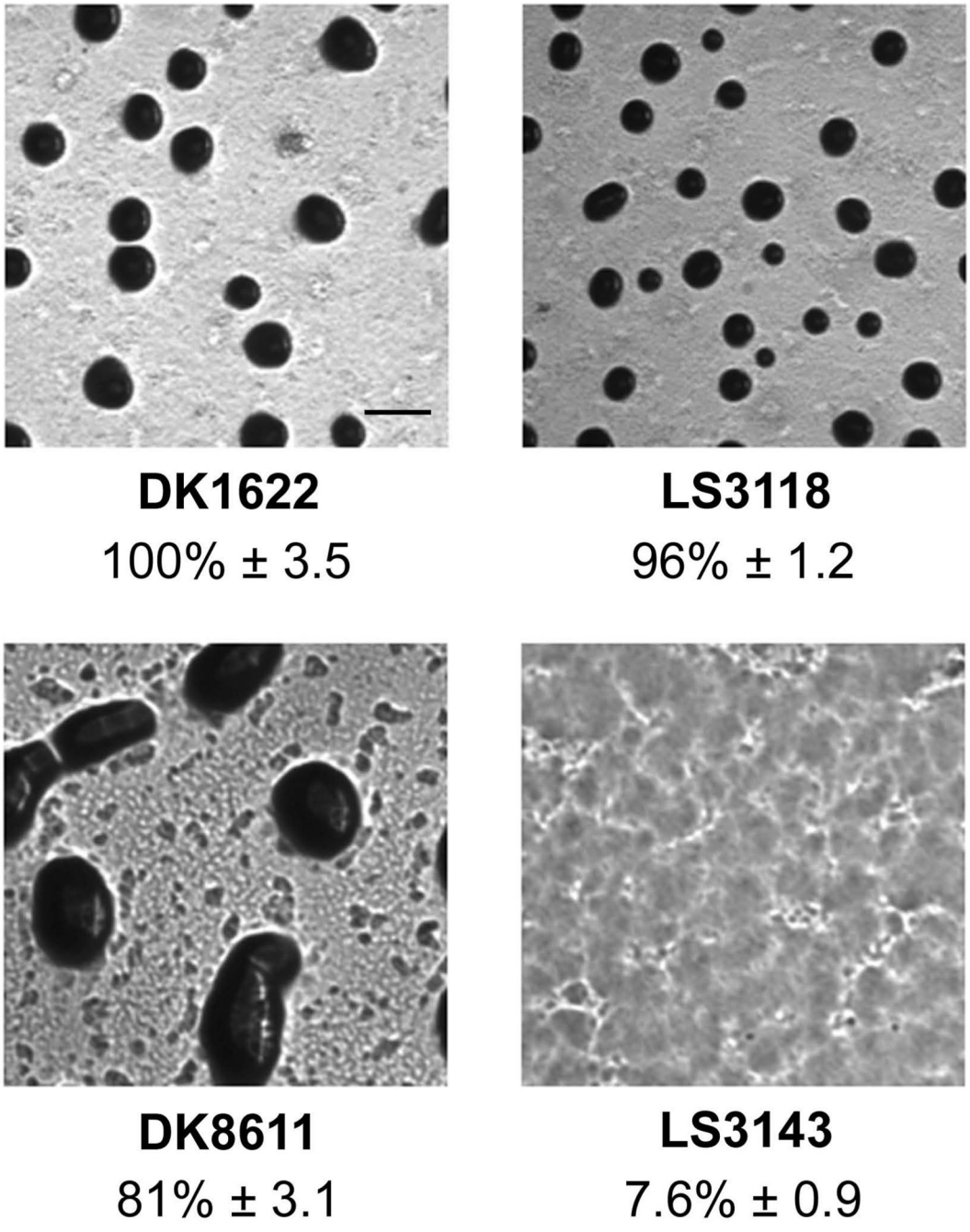

Figure 5.
Effect of *mazF* removal on fruiting body formation. Deletion of *mazF* (LS3118) has no effect on fruiting body formation compared to wild type DK1622. The *pilQ1* mutant (DK8611) is also able to form fruiting bodies. Only when both mutations are present (LS3143) is fruiting body development impaired. All images are taken approximately 48 hours post-initiation under equal magnification. % sporulation relative to DK1622 is given beneath each photograph ± standard deviation. Black bar = 200 μm.

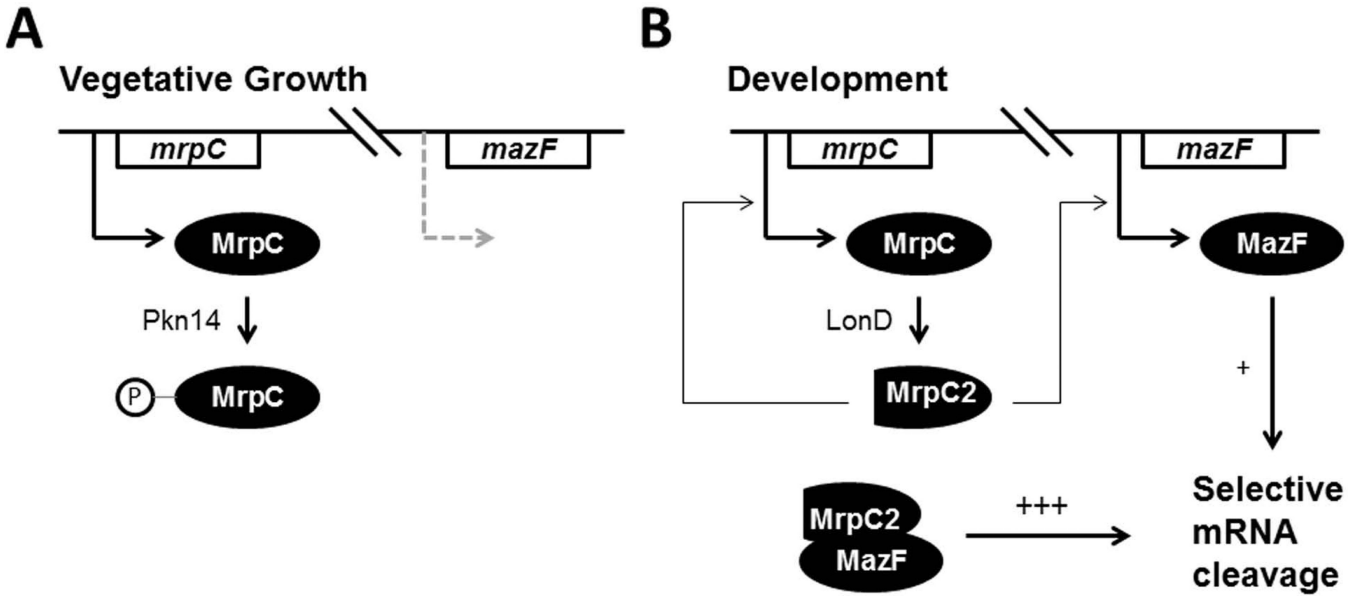

Figure 6.

Model of MazF function. **A.** During vegetative growth, MrpC phosphorylation by Pkn14 renders it unable to activate transcription of MazF. **B.** Upon starvation, MrpC is cleaved to MrpC2 directly or indirectly by protease LonD and can no longer be phosphorylated. MrpC and MazF expression are upregulated and the interaction of MazF and MrpC leads to mRNA interferase activity.

Table 1

Bacterial strains and plasmids used in the course of this study.

Strain or Plasmid	Description	Reference
Strains		
E. coli		
DH10B	Used for cloning of plasmids and protein expression	(Durfee *et al.*, 2008)
M. xanthus		
DK1622	Wild-type strain	(Chen *et al.*, 1990)
LS3118	DK1622 bearing a clean deletion of *mazF*	This study
DK8611	DK1622 bearing the *pilQ1* allele	(Wall et al., 1999)
LS3143	DK1622 bearing both LS3118 and DK8611 mutations	This study
LS3160	DK1622 bearing two silent mutations, T751C and G753C in the *nla6* (MXAN4042) gene	This study
Plasmids		
pUC57	Derivative of pUC19, *E. coli* vector	(Yanisch-Perron *et al.*, 1985)
pTOB12	Synthetic clone of *M. xanthus mazF* (MXAN1659) flanking regions inserted into pUC57	This study
pBJ113	*M. xanthus* recombination backbone plasmid	(Ueki et al., 1996)
pTOB13	pBJ113 containing inserted sequence of pTOB12	This study
pTOB1	Synthetic clone of *M. xanthus mazF* codon optimized for *E. coli* inserted into pUC57	This study
pTrcHisB	*E. coli* Expression vector	(Amann *et al.*, 1983)
pTOB2	Codon optimized *mazF* sequence inserted into pTrcHisB	This study
pTOB7	Synthetic clone of *M. xanthus mrpC* (MXAN5125) codon optimized for *E. coli* inserted into pUC57	
pTYB2	*E. coli* Expression vector	(Chong *et al.*, 1997)
pTOB14	Codon optimized *mrpC* sequence inserted in pTYB2	This study
pTOB15	Codon optimized *mrpC2* sequence inserted in pTYB2	This study
pTOB30	pBJ113 containing *nla6* (MXAN4042) bearing T751C and G753C mutations	